

NUCLEAR DATA AND MEASUREMENTS SERIES

ANL/NDM-102

**Investigation of the Influence of the Neutron Spectrum in
Determinations of Integral Neutron Cross-Section Ratios**

by

Donald L. Smith

November 1987

**ARGONNE NATIONAL LABORATORY,
ARGONNE, ILLINOIS 60439, U.S.A.**

NUCLEAR DATA AND MEASUREMENTS SERIES

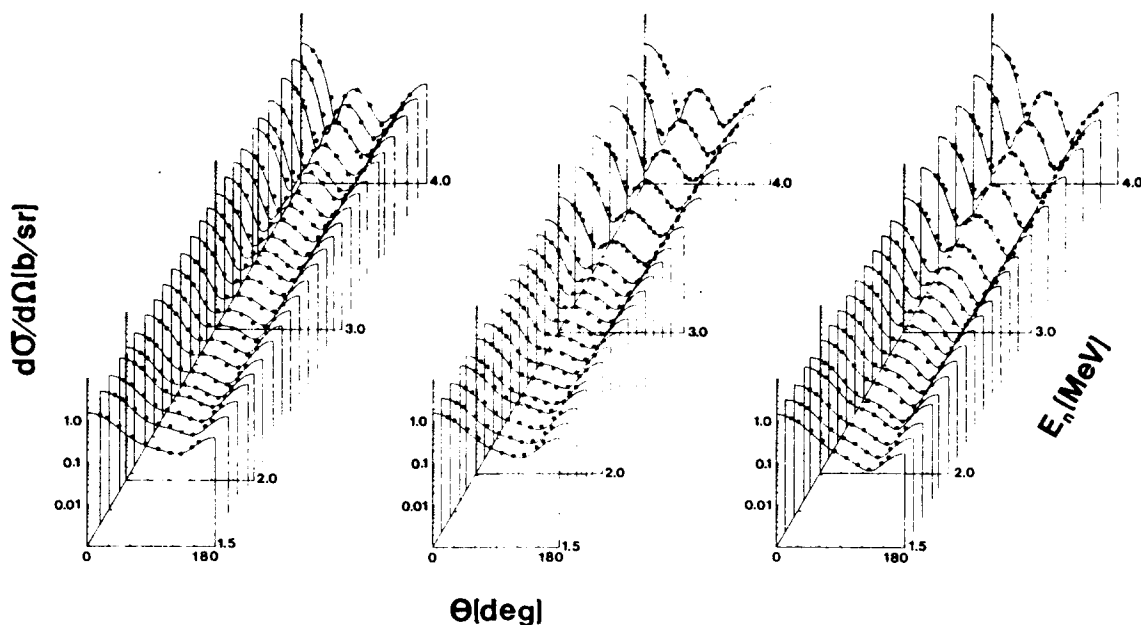
ANL/NDM-102

INVESTIGATION OF THE INFLUENCE OF THE
NEUTRON SPECTRUM IN DETERMINATIONS OF
INTEGRAL NEUTRON CROSS-SECTION RATIOS*

by

Donald L. Smith

November 1987



ARGONNE NATIONAL LABORATORY, ARGONNE, ILLINOIS

Operated by THE UNIVERSITY OF CHICAGO

for the U. S. DEPARTMENT OF ENERGY

under Contract W-31-109-Eng-38

Argonne National Laboratory, with facilities in the states of Illinois and Idaho, is owned by the United States government, and operated by The University of Chicago under the provisions of a contract with the Department of Energy.

DISCLAIMER

This report was prepared as an account of work sponsored by an agency of the United States Government. Neither the United States Government nor any agency thereof, nor any of their employees, makes any warranty, express or implied, or assumes any legal liability or responsibility for the accuracy, completeness, or usefulness of any information, apparatus, product, or process disclosed, or represents that its use would not infringe privately owned rights. Reference herein to any specific commercial product, process, or service by trade name, trademark, manufacturer, or otherwise, does not necessarily constitute or imply its endorsement, recommendation, or favoring by the United States Government or any agency thereof. The views and opinions of authors expressed herein do not necessarily state or reflect those of the United States Government or any agency thereof.

ANL/NDM-102

INVESTIGATION OF THE INFLUENCE OF THE
NEUTRON SPECTRUM IN DETERMINATIONS OF
INTEGRAL NEUTRON CROSS-SECTION RATIOS*

by

Donald L. Smith

November 1987

NEUTRON CROSS-SECTION DATA ANALYSIS. Integral cross-section ratios. Quasi-monoenergetic cross-section ratios. Differential cross-section energy dependence. Neutron-spectrum moments. Covariance matrices. Error propagation. Cross-section ratio data correction.

Applied Physics Division
Argonne National Laboratory
9700 South Cass Avenue
Argonne, Illinois 60439
U.S.A.

*This work supported by the U.S. Department of Energy, Energy Research Programs, under contract W-31-109-Eng-38.

NUCLEAR DATA AND MEASUREMENTS SERIES

The Nuclear Data and Measurements Series presents results of studies in the field of microscopic nuclear data. The primary objective is the dissemination of information in the comprehensive form required for nuclear technology applications. This Series is devoted to: a) measured microscopic nuclear parameters, b) experimental techniques and facilities employed in measurements, c) the analysis, correlation and interpretation of nuclear data, and d) the evaluation of nuclear data. Contributions to this Series are reviewed to assure technical competence and, unless otherwise stated, the contents can be formally referenced. This Series does not supplant formal journal publication but it does provide the more extensive information required for technological applications (e.g., tabulated numerical data) in a timely manner.

Copies on microfiche can be obtained by contacting:

National Technical Information Service
U.S. Department of Commerce
5285 Port Royal Road
Springfield, Virginia 22161
U.S.A.

INFORMATION ABOUT OTHER ISSUES IN THE ANL/NDM SERIES

A list of titles and authors for reports ANL/NDM-1 through ANL/NDM-50 can be obtained by referring to any report of this Series numbered ANL/NDM-51 through ANL/NDM-76, while those for ANL/NDM-51 through ANL/NDM-76 are listed in any report numbered ANL/NDM-77 through ANL/NDM-101. Requests for a complete list of titles or for copies of previous reports should be directed to:

Section Secretary
Applied Nuclear Physics Section
Applied Physics Division
Building 316
Argonne National Laboratory
9700 South Cass Avenue
Argonne, Illinois 60439
U.S.A.

ANL/NDM-76 Alan B. Smith and Peter T. Guenther, *Scattering of Fast Neutrons from Elemental Molybdenum*, November 1982.

ANL/NDM-77 Donald L. Smith, *A Least-squares Method for Deriving Reaction Differential Cross Section Information from Measurements Performed in Diverse Neutron Fields*, November 1982.

ANL/NDM-78 A.B. Smith, P.T. Guenther and J.F. Whalen, *Fast-neutron Total and Elastic-scattering Cross Sections of Elemental Indium*, November 1982.

ANL/NDM-79 C. Budtz-Joergensen, P. Guenther, A. Smith and J. Whalen, *Few-MeV Neutrons Incident on Yttrium*, June 1983.

ANL/NDM-80 W.P. Poenitz and J.F. Whalen, *Neutron Total Cross Section Measurements in the Energy Region from 47 keV to 20 MeV*, July 1983.

ANL/NDM-81 D.L. Smith and P.T. Guenther, *Covariances for Neutron Cross Sections Calculated Using a Regional Model Based on Elemental-model Fits to Experimental Data*, November 1983.

ANL/NDM-82 D.L. Smith, *Reaction Differential Cross Sections from the Least-squares Unfolding of Ratio Data Measured in Diverse Neutrons Fields*, January 1984.

ANL/NDM-83 J.W. Meadows, *The Fission Cross Sections of Some Thorium, Uranium, Neptunium and Plutonium Isotopes Relative to ^{235}U* , October 1983.

ANL/NDM-84 W.P. Poenitz and J.W. Meadows, *^{235}U and ^{239}Pu Sample-mass Determinations and Intercomparisons*, November 1983.

- ANL/NDM-85 D.L. Smith, J.W. Meadows and I. Kanno, *Measurement of the $^{51}\text{V}(n,p)^{51}\text{Ti}$ Reaction Cross Section from Threshold to 9.3 MeV*, June 1984.
- ANL/NDM-86 I. Kanno, J.W. Meadows and D.L. Smith, *Energy-differential Cross-section Measurement for the $^{51}\text{V}(n,\alpha)^{48}\text{Sc}$ Reaction*, July 1984.
- ANL/NDM-87 D.L. Smith, J.W. Meadows, M.M. Bretscher and S.A. Cox, *Cross-section Measurement for the $^7\text{Li}(n,n't)^4\text{He}$ Reaction at 14.74 MeV*, September 1984.
- ANL/NDM-88 A.B. Smith, D.L. Smith and R.J. Howerton, *An Evaluated Nuclear Data File for Niobium*, March 1985.
- ANL/NDM-89 Bernard P. Evain, Donald L. Smith and Paul Lucchese, *Compilation and Evaluation of 14-MeV Neutron-activation Cross Sections for Nuclear Technology Applications: Set I*, April 1985.
- ANL/NDM-90 D.L. Smith, J.W. Meadows and P.T. Guenther, *Fast-neutron-spectrum Measurements for the Thick-target $^9\text{Be}(d,n)^{10}\text{B}$ Reaction at $E_d = 7$ MeV*, April 1985.
- ANL/NDM-91 A.B. Smith, P.T. Guenther and R.D. Lawson, *On the Energy Dependence of the Optical Model of Neutron Scattering from Niobium*, May 1985.
- ANL/NDM-92 Donald L. Smith, *Nuclear Data Uncertainties (Vol.-I): Basic Concepts of Probability*, April 1986.
- ANL/NDM-93 D.L. Smith, J.W. Meadows and M.M. Bretscher, *Integral Cross-section Measurements for $^7\text{Li}(n,n't)^4\text{He}$, $^{27}\text{Al}(n,p)^{27}\text{Mg}$, $^{27}\text{Al}(n,\alpha)^{24}\text{Na}$, $^{58}\text{Ni}(n,p)^{58}\text{Co}$ and $^{60}\text{Ni}(n,p)^{60}\text{Co}$ Relative to ^{238}U Neutron Fission in the Thick-target $^9\text{Be}(d,n)^{10}\text{B}$ Spectrum at $E_d = 7$ MeV*, October 1985.
- ANL/NDM-94 A.B. Smith, D.L. Smith, P. Rousset, R.D. Lawson and R.J. Howerton, *Evaluated Neutronic Data File for Yttrium*, January 1986.
- ANL/NDM-95 Donald L. Smith and James W. Meadows, *A Facility for High-intensity Neutron Irradiations Using Thick-target Sources at the Argonne Fast-neutron Generator*, May 1986.

ANL/NDM-96 M. Sugimoto, A.B. Smith and P.T. Guenther, *Ratio of the Prompt-fission-neutron Spectrum of Plutonium-239 to that of Uranium-235*, September 1986.

ANL/NDM-97 J.W. Meadows, *The Fission Cross Sections of ^{230}Th , ^{232}Th , ^{233}U , ^{234}U , ^{236}U , ^{238}U , ^{237}Np , ^{239}Pu and ^{242}Pu Relative ^{235}U at 14.74 MeV Neutron Energy*, December 1986.

ANL/NDM-98 J.W. Meadows, *The Fission Cross Section Ratios and Error Analysis for Ten Thorium, Uranium, Neptunium and Plutonium Isotopes at 14.74-MeV Neutron Energy*, March 1987.

ANL/NDM-99 Donald L. Smith, *Some Comments on the Effects of Long-range Correlations in Covariance Matrices for Nuclear Data*, March 1987.

ANL/NDM-100 A.B. Smith, P.T. Guenther and R.D. Lawson, *The Energy Dependence of the Optical-model Potential for Fast-neutron Scattering from Bismuth*, May 1987.

ANL/NDM-101 A.B. Smith, P.T. Guenther, J.F. Whalen and R.D. Lawson, *Cobalt: Fast Neutrons and Physical Models*, July 1987.

TABLE OF CONTENTS

	<u>Page</u>
ABSTRACT	1
I. INTRODUCTION	2
II. MONOENERGETIC RATIOS	3
III. INTEGRAL RATIOS	10
IV. CONCLUSIONS	19
ACKNOWLEDGEMENTS	20
REFERENCES	21
TABLES	23
FIGURE	27

INVESTIGATION OF THE INFLUENCE OF THE
NEUTRON SPECTRUM IN DETERMINATIONS OF
INTEGRAL NEUTRON CROSS-SECTION RATIOS*

by

Donald L. Smith

Applied Physics Division
Argonne National Laboratory
9700 South Cass Avenue
Argonne, Illinois 60439
U.S.A.

ABSTRACT

Ratio measurements are routinely employed in studies of neutron interaction processes in order to generate new differential cross-section data or to test existing differential cross-section information through examination of the corresponding response in integral neutron spectra. Interpretation of such data requires that careful attention be given to details of the neutron spectra involved in these measurements. Two specific tasks are undertaken in the present investigation: i) Using perturbation theory, a formula is derived which permits one to relate the ratio measured in a realistic quasi-monoenergetic spectrum to the desired pure monoenergetic ratio. This expression involves only the lowest-order moments of the neutron energy distribution and corresponding parameters which serve to characterize the energy dependence of the differential cross sections, quantities which can generally be estimated with reasonable precision from the uncorrected data or from auxiliary information. ii) Using covariance methods, a general formalism is developed for calculating the uncertainty of a measured integral cross-section ratio which involves an arbitrary neutron spectrum. This formalism is employed to further examine the conditions which influence the sensitivity of such measured ratios to details of the neutron spectra and to their uncertainties. Several numerical examples are presented in this report in order to illustrate these principles, and some general conclusions are drawn concerning the development and testing of neutron cross-section data by means of ratio experiments.

*This work supported by the U.S. Department of Energy, Energy Research Programs, under contract W-31-109-Eng-38.

I. INTRODUCTION

In experimental neutron nuclear data research the development of cross section information has conventionally progressed largely along two lines, namely differential measurements for use in the production of energy-dependent evaluated cross-section data files (e.g., ENDF/B-V [1]) and integral measurements for use in testing existing evaluated differential information. Recently, techniques have been developed and occasionally applied which enable differential and integral information to be combined in a unified fashion within the framework of the evaluation process itself (e.g., Ref. 2 and 3). However, the more conventional approach continues to be pursued by a majority of researchers in the field.

Ratio measurements play a very important role in this data development process. First and foremost, ratio measurements permit investigators to avoid the difficult issue of absolute neutron fluence determination by allowing them to reference their measurements to standards which are presumed to be well known, or at least are well documented and widely acknowledged. Another appealing feature of ratio measurements is that the results of such measurements are sometimes found to be rather insensitive to particular details of the neutron fields in which these measurements are performed. For example, it is generally found that monoenergetic measurements are not very sensitive to properties of the neutron spectrum except in those cases where pronounced resonance structure is involved. For integral measurements in neutron spectra with broad energy ranges, the results of ratio measurements have also been found to be relatively insensitive to details of the spectrum shape under certain restrictive conditions, e.g., when the excitation functions for the cross-sections in question are relatively flat over a wide energy range (such as for U-235 and Pu-239 fast-neutron fission) or when they exhibit similar threshold behavior. Although these observations are widely accepted within the community of nuclear data researchers, it appears that little formal effort has been expended to investigate the matter in any quantitative detail.

The present investigation was undertaken to address the following two specific issues which fall within this category: i) The relationship between a ratio measured in a realistic quasi-monoenergetic neutron spectrum and the idealized pure monoenergetic ratio is derived (in Chapter II). ii) The sensitivity of a measured integral ratio to the shape and assumed uncertainties of a neutron spectrum with arbitrary energy dependence is examined (in Chapter III). Examples are presented in both instances to illustrate the developed formalism. Conclusions reached from this work are discussed in Chapter IV.

II. MONOENERGETIC RATIOS

The importance of monoenergetic ratio data is evident from the following considerations: Let $R(E) = \sigma_2(E)/\sigma_1(E)$ be the ratio of two neutron reaction differential cross sections at a particular energy E , such that σ_1 represents a standard cross section which is well known as a function of neutron energy and σ_2 is the cross section for a reaction which is less well known. The ratio can be measured without having to determine the absolute neutron fluence, and therefore it can in practice be determined with much better accuracy through direct determination than the cross sections themselves. Solving for σ_2 , one obtains the formula $\sigma_2(E) = R(E)\sigma_1(E)$. Thus, the differential cross section σ_2 for the less-well-known reaction can in principle be deduced from the measured ratio and prior knowledge of the standard cross section σ_1 . This, in fact, is the most widely employed procedure in the field of nuclear data for experimentally determining neutron reaction cross sections.

However, there is an important complication. While the measurement of the ratio is not dependent upon absolute fluence (total number of neutrons involved in the irradiations), there is unavoidable dependence upon the neutron energy spectrum (i.e., the actual distribution in energy of the incident neutrons). In fact, when one measures the ratio in a realistic experiment, what one observes physically is the quantity R_m given by the formula:

$$(1) \quad R_m = G_2/G_1 = \int \phi(E)\sigma_2(E)dE / \int \phi(E)\sigma_1(E)dE,$$

where the neutron spectrum is represented by the continuous function ϕ and the integrals symbolically represent summation over the entire energy range spanned by the spectrum. For convenience, we assume that the spectrum is normalized, i.e., that $\int \phi(E)dE = 1$.

In an idealized monoenergetic experiment at energy E_0 , the spectrum could be represented by the function $\phi(E) = \delta(E-E_0)$, where δ is the Dirac delta function. Substitution of this representation of ϕ into Eq. 1 yields the relationship $R_m = \sigma_2(E_0)/\sigma_1(E_0)$. Thus the measured ratio R_m is equivalent to the idealized monoenergetic ratio, designated $R_0 = R(E_0)$ in this circumstance.

For spectra employed in actual "monoenergetic" measurements, the neutrons do tend to have energies which are confined to the vicinity of the selected measurement energy E_0 . Variance in the distribution ϕ is kept as small as possible, consistent with the realities of experimental procedure, but is never vanishingly small (i.e., the

measurement resolution is finite). A more descriptive label for such measurements would be "quasi-monoenergetic". Some of the implications of dispersion in neutron cross section measurements have been addressed previously [4]. The procedure discussed in this earlier work could be applied to the analysis of cross-section ratio data. In particular, the ideal monoenergetic ratio R_0 could be "factored" from Eq. 1 as follows:

$$(2) \quad R_m = R_0 \left\{ \int \phi(E) [\sigma_2(E)/\sigma_{20}] dE / \int \phi(E) [\sigma_1(E)/\sigma_{10}] dE \right\},$$

where $\sigma_{10} = \sigma_1(E_0)$, $\sigma_{20} = \sigma_2(E_0)$ and $R_0 = \sigma_{20}/\sigma_{10}$. A serious limitation of this procedure is that it requires that the shapes of the cross sections and spectrum as a function of energy be specified in detail so that the indicated integrals can be computed. Although knowledge of these shapes can be approximate, and they can be estimated from prior information (e.g., from evaluated files such as ENDF/B-V [1] for the cross sections and from models of the neutron production mechanism for the spectrum [5-7]), this limitation can be rather troublesome and restrictive in many applications.

The objective here is to find a method for deriving the true monoenergetic cross-section ratio R_0 from the measured ratio R_m through the application of a correction involving a minimum number of parameters which can be estimated, either from prior information or from the raw data. Let us define the energy E_0 as the mean value of the neutron distribution $\phi(E)$, that is

$$(3) \quad E_0 = \int E \phi(E) dE.$$

We then generate Taylor's series expansions for the cross sections σ_1 and σ_2 relative to E_0 , i.e.,

$$(4) \quad \sigma_1(E) \approx \sigma_{10} + \sum_{k=1}^n f_{1k} (E-E_0)^k / k!,$$

$$(5) \quad \sigma_2(E) \approx \sigma_{20} + \sum_{k=1}^n f_{2k} (E-E_0)^k / k!.$$

where f_{1k} and f_{2k} are derivatives of order k for σ_1 and σ_2 , respectively, evaluated at E_0 . That is $f_{1k} = d^k \sigma_1(E_0) / dE^k$ and $f_{2k} = d^k \sigma_2(E_0) / dE^k$. This procedure is a reasonable one only if the variance in the neutron spectrum is considerably smaller than the energy range over which significant variations are anticipated for the cross-section excitation functions. In particular, sharp resonances narrower than the neutron spectrum cannot be tolerated.

Consideration of Eqs. 1, 4 and 5, leads to the expressions

$$(6) \quad G_1 \approx \sigma_{10} + \sum_{k=1}^n f_{1k} \mu_k / k!$$

$$(7) \quad G_2 \approx \sigma_{20} + \sum_{k=1}^n f_{2k} \mu_k / k!,$$

where

$$(8) \quad \mu_k = \int \phi(E) (E - E_0)^k dE \quad (k = 1, n).$$

The parameter μ_k has special meaning in a statistical context. It represents the k -th central moment of the neutron spectrum. The number of terms (n) in the expansion which are necessary in order to provide a good approximation depends strongly on the nature of the cross sections and the spectrum, but in most instances a few terms ($n \leq 4$) should suffice.

Much is known about the nature of the various moments μ_k (see Ref. 8). For example, it is evident that $\mu_1 = 0$ from the definition of E_0 in Eq. 3. Furthermore, the moment μ_2 is identified as the variance of E for the spectrum ϕ . It is a measure of the extent or "width" of the spectrum. Better known is the standard deviation, s (we avoid the use of the more conventional notation σ in order to avoid confusion with cross section), which is related to μ_2 by the expression $\mu_2 = s^2$. The next two higher-order moments are also used to describe certain physical properties of the spectrum. The parameter $\alpha = \mu_3/s^3$ is commonly known as the skewness of the neutron distribution ϕ , relative to the mean energy E_0 . Negative values of α imply that the spectrum is skewed toward lower energies while positive values of α indicate that it is skewed toward higher energies. A symmetric distribution is indicated if $\alpha = 0$. Most realistic quasi-monoenergetic neutron distributions encountered in practice are skewed toward lower energies ($\alpha < 0$) [4-7]. Finally, the parameter $\beta = \mu_4/s^4$ is known as the kurtosis of the distribution (it is always positive). Comparison is usually made relative to a pure Gaussian distribution for which $\beta = 3$ (Mesokurtic). If $\beta > 3$ (Leptokurtic), the distribution is more strongly "peaked" than a Gaussian with similar variance while $\beta < 3$ (Platykurtic) implies a "flatter" shape than a comparable Gaussian.

The fact that the influence of the spectrum in a quasi-monoenergetic ratio measurement can be examined in terms of a few well-defined "statistical" parameters associated with the spectrum is of considerable practical importance. It is quite reasonable to assume that an experienced investigator can produce adequate estimates for these few parameters from a consideration of the neutron production process in his experiment; however, it is asking much more to expect him to generate a comprehensive energy-dependent representation $\phi(E)$, as required for the correction procedure indicated by Eq. 2.

A minor modification of Eqs. 6 and 7 yields the expressions

$$(9) \quad G_1 \approx \sigma_{10} \left(1 + \sum_{k=2}^n g_{1k} \mu_k / k! \right)$$

$$(10) \quad G_2 \approx \sigma_{20} \left(1 + \sum_{k=2}^n g_{2k} \mu_k / k! \right),$$

where $g_{1k} = f_{1k}/\sigma_{10}$ and $g_{2k} = f_{2k}/\sigma_{20}$. Note that only terms for $k \geq 2$ need to be considered in the sums owing to the fact that $\mu_1 = 0$. These terms are normally anticipated to be considerably smaller than unity, and in many instances they become progressively smaller with increasing k . From the preceding equations we are led to the following approximate relationship between R_m and R_0 .

$$(11) \quad R_m \approx R_0 \left[1 + \sum_{k=2}^n (g_{2k} - g_{1k}) \mu_k / k! \right].$$

This approximation can become quite precise if sufficient terms are included in the sum, and if the estimates of the parameters g_{1k} , g_{2k} and μ_k are reasonable. For present purposes it will be assumed that the approximation is adequate for $n = 4$. Then, using the definitions given above, Eq. 11 can be rewritten in the following interesting form:

$$(12) \quad R_m \approx R_0 \left[1 + (g_{22} - g_{12}) s^2 / 2! + (g_{23} - g_{13}) \alpha s^3 / 3! \right. \\ \left. + (g_{24} - g_{14}) \beta s^4 / 4! \right].$$

The first correction term arises as a result of spread in the spectrum (the variance). The second term contributes if the spectrum is skewed; however, it vanishes if the spectrum is symmetric with respect to the mean energy E_0 . Finally, the contribution from the third term is affected by whether the spectrum tends towards a flat shape or is locally sharply-peaked in the vicinity of E_0 .

In order to examine the influence of the cross sections in the correction process, it is necessary to consider the parameters g_{1k} and g_{2k} . Estimates of these must be provided in order to apply the formalism. Some suggestions as to how this can be accomplished in practice are offered in the following paragraphs.

Since it is assumed that the standard cross section σ_1 in the vicinity of E_0 is adequately known, the major concern is with σ_2 . If some prior information on the latter is available from previous experiments or from an evaluation based on data, models, etc., then it may very well serve this purpose adequately. Otherwise, the necessary information can in principle be deduced from uncorrected experimental ratio data acquired at various energies in the vicinity of E_0 . Estimates of the shape of σ_2 can be deduced by combining these data with standard cross section values according to the well-known formula stated above. So, it is evident that there is a price to pay for acquiring a refined knowledge of the ratio at a particular energy. The price is that data must be obtained at neighboring energies in order to permit estimation of the derivatives appearing in the Taylor's series expansion. Since this can generally be accomplished in a straightforward manner, there do not appear to exist any insurmountable obstacles associated with application of the present method.

We shall assume that some information on the energy dependence of σ_1 and σ_2 is available (as discussed above). A reasonable way to proceed is to represent this information by simple polynomial expansions of the following form:

$$(13) \sigma_1(E) \approx \sigma_{10} + \sum_{k=1}^n a_{1k} (E-E_0)^k,$$

$$(14) \sigma_2(E) \approx \sigma_{20} + \sum_{k=1}^n a_{2k} (E-E_0)^k.$$

The parameters a_{1k} and a_{2k} can be deduced by least-squares fitting to the available shape information. Furthermore, from an inspection of Eqs. (4), (5), (13) and (15) it is evident that these a_{1k} and a_{2k} parameters are closely related to the derivatives f_{1k} and f_{2k} which appear in the preceding formalism, i.e., $f_{1k} = k!a_{1k}$ and $f_{2k} = k!a_{2k}$. Furthermore, $g_{1k} = k!a_{1k}/\sigma_{10}$ and $g_{2k} = k!a_{2k}/\sigma_{20}$. If we then let $h_{1k} = a_{1k}/\sigma_{10}$ and $h_{2k} = a_{2k}/\sigma_{20}$, Eqs. 11 and 12 can be rewritten as follows:

$$(15) R_m \approx R_0 \left[1 + \sum_{k=2}^n (h_{2k} - h_{1k}) \mu_k \right],$$

$$(16) R_m \approx R_0 \left[1 + (h_{22} - h_{12}) s^2 + (h_{23} - h_{13}) \alpha s^3 + (h_{24} - h_{14}) \beta s^4 \right].$$

It is also useful for some purposes to express the relationship between R_m and R_0 in the form $R_m \approx R_0 Q$, where

$$(17) Q = \left(1 + \sum_{k=2}^n t_k \right).$$

The significance of the factors t_k is obvious from Eq. 17 since the desired correction factor Q is simply unity plus the sum of these terms.

Example 1

This example will serve to illustrate the concepts presented in this chapter. A realistic spectrum shape has been generated using the procedure described by Smith and Meadows [5]. This represents the spectrum of ${}^2\text{H}(d,n){}^3\text{He}$ neutrons produced via 3-MeV deuteron bombardment of a target cell containing deuterium gas. Table 1 provides a discrete representation of this spectrum in neutron-energy increments of 13-14 keV. The essential parameters of the spectrum (defined in terms of integrals in the formalism) are computed for this example by the method

of finite sums, e.g., $E_0 \approx \sum_{i=1}^{29} E_i \phi_i = 5.841$ MeV. The moments of concern

in this example are the following: $\mu_2 \approx 5.851 \times 10^{-3}$ MeV² (standard deviation $s \approx 0.0765$ MeV), $\mu_3 \approx -2.036 \times 10^{-4}$ MeV³ (skewness $\alpha \approx -0.455$) and $\mu_4 \approx 9.131 \times 10^{-5}$ MeV⁴ (kurtosis $\beta \approx 2.67$). The spectrum is therefore somewhat "flatter" than a comparable Gaussian, and it has a low-energy tail (skewed toward lower values of neutron energy).

For the purposes of this example, the cross sections in the vicinity of $E_0 = 5.841$ MeV are represented by the following polynomial parameters (in accordance with Eqs. 13 and 14):

σ_1

$$\begin{aligned}\sigma_{10} &= 200 \text{ millibarn} \\ a_{11} &= 100 \text{ millibarn MeV}^{-1} \\ a_{12} &= 500 \text{ millibarn MeV}^{-2} \\ a_{13} &= 2500 \text{ millibarn MeV}^{-3} \\ a_{14} &= 12500 \text{ millibarn MeV}^{-4}\end{aligned}$$

 σ_2

$$\begin{aligned}\sigma_{20} &= 100 \text{ millibarn} \\ a_{21} &= -50 \text{ millibarn MeV}^{-1} \\ a_{22} &= -250 \text{ millibarn MeV}^{-2} \\ a_{23} &= 1250 \text{ millibarn MeV}^{-3} \\ a_{24} &= -6250 \text{ millibarn MeV}^{-4}\end{aligned}$$

For this choice, each of the terms in Eqs. 13 and 14 contributes no more than 10% to the cross section variations with energy (relative to the values at E_0) over the range of the spectrum ϕ . Plots of σ_1 , σ_2 and ϕ are provided in Fig. 1. From this figure it is evident that the energy point $E_0 = 5.841$ MeV falls near a "resonance" minimum for σ_1 and near a "resonance" maximum for σ_2 . Furthermore, the variation with energy of these cross sections (over the spectrum range) is moderate, thereby insuring applicability of the present procedure.

The results of the analysis based on these input data are as follows: $R_0 = 0.5$, $Q \approx 0.9593$ [based on $t_2 \approx -0.02926$ ($\geq 2.9\%$), $t_3 = 0$ and $t_4 \approx 0.01141$ ($\geq 1.1\%$)] and $R_m \approx 0.4800$. Note that even though the spectrum is skewed, t_3 is zero because of the specific nature of the cross sections which results in $h_{23} = h_{13}$. The product $R_0 Q$ differs from R_m by only 0.07%; however, it should be noted that in this particular simulation exercise the moments of ϕ and the derivatives of σ_1 and σ_2 are precisely determined from the assumed hypothetical representations of these energy dependent quantities. The spectrum and cross-section shapes appearing in this example are typical of what might be encountered in experiments involving fluctuating cross sections (e.g., in the resolved resonance region). The correction here amounts to some 4%, certainly a non-negligible effect for many purposes.

III. INTEGRAL RATIOS

When the neutron spectrum employed in a measurement is relatively broad, e.g., a reactor spectrum, one resulting from natural radioactivity or one produced at an accelerator (see Ref. 9), the procedures discussed in Chapter II are no longer relevant. Nevertheless, the extent to which the interpretation of results from such a measurement depends upon detailed knowledge of the spectrum continues to be a matter of critical importance. At present, probably only one neutron spectrum is sufficiently reproducible and well-characterized to be considered a true "benchmark" field, namely that one arising from the spontaneous fission of ^{252}Cf [10]. In general, the level of quantitative understanding of the other neutron environments which are routinely employed for neutron nuclear data development and testing purposes is limited to an extent where serious difficulty is routinely encountered in the analysis of data. This is a problem with which the nuclear data community must cope for the foreseeable future.

In this chapter, the influence of uncertainties in broad-spectrum representations on the interpretation of integral cross-section ratio data will be examined using covariance methods [11]. The objective is to establish a formalism which can be used to analyze quantitatively the impact of integral ratio data in either the development or testing of differential cross section representations for specific reactions.

Eq. 1 forms the basis for a treatment of this problem. However, in the present chapter continuous representations of the spectrum and differential cross-section functions are abandoned in favor of group representations, as is the normal procedure for most reactor physics analyses. Identical group structures are used to represent the spectrum and two cross sections. The number of groups is indicated by the integer n . The physical quantities are represented by $(1,n)$ row vectors

$$\bar{\sigma}_1^+ = (\sigma_{11}, \sigma_{12}, \dots, \sigma_{11}, \dots, \sigma_{1n}),$$

$$\bar{\sigma}_2^+ = (\sigma_{21}, \sigma_{22}, \dots, \sigma_{21}, \dots, \sigma_{2n}),$$

$$\bar{\phi}^+ = (\phi_1, \phi_2, \dots, \phi_1, \dots, \phi_n),$$

where the bar over a quantity denotes a vector and "+" indicates transposition (in this case from $(n,1)$ column vectors).

Using this matrix notation, Eq. 1 can be written in the form

$$(18) R = G_2/G_1 = (\bar{\phi}^+ \bar{\sigma}_2) / (\bar{\phi}^+ \bar{\sigma}_1).$$

The subscript "m" has been excluded for a reason. In this chapter we choose to consider R as a quantity which is calculated from the indicated physical parameters, in contrast with R_m which we consider to represent a true measured value to be compared with R . We also choose to explicitly emphasize the functional nature of R , i.e., $R = R(\bar{\sigma}_1, \bar{\sigma}_2, \bar{\phi})$. Then, let \bar{x} represent the combined array of these physical quantities, namely a $(3n, 1)$ column vector. It can be conveniently written here in the transpose form, $\bar{x}^+ = (\bar{\sigma}_1^+, \bar{\sigma}_2^+, \bar{\phi}^+)$. Then, $R = R(\bar{x})$.

The problem is therefore to develop an expression for the uncertainty in R in terms of the uncertainty in \bar{x} (that is in the spectrum and in the differential cross sections as well). The rule of error propagation [11] is applicable in this context. Here, it assumes the form

$$(19) E_R^2 = \bar{T}^+ \bar{V}_x \bar{T},$$

where E_R is the uncertainty in R , \bar{V}_x is the $(3n, 3n)$ covariance matrix applicable to \bar{x} , and \bar{T} is the $(3n, 1)$ transformation matrix, or, as it is more commonly designated, the sensitivity matrix. \bar{V}_x is generally partitioned into submatrices, and the manner in which this is done depends upon those physical assumptions which are made concerning the correlations reflected in this matrix. For the present treatment, it will be assumed that no correlations exist between the spectrum uncertainties and those related to the differential cross sections. This is an assumption which appears to be applicable, at least to a good approximation, in a wide variety of important applied problems. In general, it should not be assumed that there are no correlations between the uncertainties for the two differential cross sections appearing in the ratio. Thus, we can express \bar{V}_x in the form

$$(20) \bar{V}_x = \begin{bmatrix} \bar{V}_\sigma & 0 \\ 0 & \bar{V}_\phi \end{bmatrix},$$

where "0" denotes zero off-diagonal submatrices. The sensitivity matrix \bar{T} must then be correspondingly partitioned. Thus,

$$(21) \bar{T} = \begin{bmatrix} \bar{T}_\sigma \\ \bar{T}_\phi \end{bmatrix}.$$

Combination of Eqs. (19)-(21) yields the expression

$$(22) E_R^2 = [\bar{T}_\sigma^+, \bar{T}_\phi^+] \begin{bmatrix} \bar{V}_\sigma & 0 \\ 0 & \bar{V}_\phi \end{bmatrix} \begin{bmatrix} \bar{T}_\sigma \\ \bar{T}_\phi \end{bmatrix}.$$

Performance of some routine matrix algebra leads to the result

$$(23) E_R^2 = E_{R\sigma}^2 + E_{R\phi}^2 = (\bar{T}_\sigma^+ \bar{V}_\sigma \bar{T}_\sigma) + (\bar{T}_\phi^+ \bar{V}_\phi \bar{T}_\phi).$$

The two terms in Eq. 23 represent distinct sources of error from a physical point of view, and this point is emphasized by the labels selected (i.e., the error due uncertainties in the cross sections and that due to uncertainties in the spectrum). Each term will be examined in turn below.

First, consider $E_{R\phi}$. The $(n,1)$ matrix \bar{T}_ϕ consists of partial derivatives $(\partial R/\partial \phi_i)$ for $i = 1, n$. Therefore,

$$(24) E_{R\phi}^2 = \sum_{i=1}^n \sum_{j=1}^n (\partial R/\partial \phi_i) V_{\phi ij} (\partial R/\partial \phi_j),$$

where $V_{\phi ij}$ is a typical element of the spectrum covariance matrix \bar{V}_ϕ .

For present purposes it is not of concern whether the spectrum $\bar{\phi}$ is normalized. For interest, however, we digress here briefly to consider the case of a spectrum representation which by definition is always normalized. In particular, if we define $\bar{\psi}$, by the relationship $\bar{\psi} = \bar{\phi}/\xi$, where $\xi = \sum_{i=1}^n \phi_i$, then the $\bar{\psi}$ is clearly always normalized.

Furthermore, its covariance matrix \bar{V}_ψ possesses the interesting property that the elements sum to exactly zero by rows or columns, i.e., $\sum_{i=1}^n V_{\psi ij} = 0$ and $\sum_{j=1}^n V_{\psi ij} = 0$ [12].

For convenience, we choose to write Eq. 18 in the more explicit form

$$(25) R = G_2/G_1 = \left(\sum_{i=1}^n \phi_i \sigma_{2i} \right) / \left(\sum_{i=1}^n \phi_i \sigma_{1i} \right).$$

Computation of the partial derivatives appearing in \bar{T}_ϕ is then quite straightforward. The result is

$$(26) \partial R / \partial \phi_i = (G_1 \sigma_{2i} - G_2 \sigma_{1i}) / G_1^2 \text{ for } i = 1, n.$$

From Eqs. 24 and 26 we are able to derive the general result

$$(27) E_{R\phi}^2 = \left[\sum_{i=1}^n \sum_{j=1}^n (G_1 \sigma_{2i} - G_2 \sigma_{1i}) V_{\phi ij} (G_1 \sigma_{2j} - G_2 \sigma_{1j}) \right] / G_1^4.$$

While Eq. 27 provides a general algorithm for numerical computation of the error in R which can be attributed directly to the uncertainties in the spectrum, it is not a very useful relationship for acquiring an understanding of the error propagation mechanism. For this purpose, it is instructive to consider a special case, namely that where the spectrum uncertainties are uncorrelated from group to group. Then, \bar{V}_ϕ is diagonal and we may write $V_{\phi ij} = E_{\phi i}^2 \delta_{ij}$ where $E_{\phi i}$ is the error in the group flux ϕ_i and $\delta_{ij} = 1$ if $i=j$ and 0 if $i \neq j$ (the Kronecker Delta Function). Under these conditions

$$(28) E_{R\phi}^2 = \left[\sum_{i=1}^n (G_1 \sigma_{2i} - G_2 \sigma_{1i})^2 E_{\phi i}^2 \right] / G_1^4.$$

At this point we turn to consideration of three specific examples:

Example 2

Suppose that the two differential cross sections differ by only a constant factor \mathcal{P} , i.e., $\sigma_{2i} = \mathcal{P} \sigma_{1i}$ for $i=1, n$. Then $G_2 = \mathcal{P} G_1$ (or equivalently, $R = \mathcal{P}$), $G_1 \sigma_{2i} - G_2 \sigma_{1i} = 0$ for $i=1, n$ and $E_{R\phi} = 0$. In this simple example it is obvious that R is a constant which is independent of the spectrum and is therefore insensitive to the spectrum uncertainties.

Example 3

In this example, arbitrary shapes are permitted for the differential cross sections, but we do require that $G_2 \approx G_1$, namely that each has about the same spectrum average cross section for the

spectrum in question ($R \approx 1$). Then, $G_1 \sigma_{2i} - G_2 \sigma_{1i} \approx G_1 (\sigma_{2i} - \sigma_{1i})$, and

$$(29) E_{R\phi}^2 \approx \left[\sum_{i=1}^n (\sigma_{2i} - \sigma_{1i})^2 E_{\phi_i}^2 \right] / G_1^2.$$

In order to demonstrate the significance of Eq. 29, we introduce some numerical values. An 11-group spectrum and cross-section representation is employed for simplicity. Two versions of σ_2 are considered. For the first (σ_2 set A), the threshold behavior is not too widely different from σ_1 , however for the second (σ_2 set B), the threshold is considerably higher. These hypothetical cross section sets are formed so that $G_2 \approx G_1$ as required. For present purposes it is assumed that the uncorrelated uncertainty in each ϕ_i is 10%. Table 2 lists the relevant numerical values for this problem. It is evident from Eq. 29 that the calculation of $E_{R\phi}$ for σ_2 set A differs from that involving σ_2 set B only through the factors $(\sigma_{2i} - \sigma_{1i})^2$. These effectively serve to "weight" the error contributions from the various groups of the spectrum in the determination of $E_{R\phi}$. The influence of the spectrum-group error E_{ϕ_i} on $E_{R\phi}$ is enhanced whenever the corresponding difference between σ_1 and σ_2 becomes large, particularly if the group is strongly represented in the spectrum. If the uncertainties in the spectrum vary widely from group to group on a percentage basis (not a consideration in the present example), then this additional factor has to be taken into consideration. In the present problem, the errors $E_{R\phi}$ (expressed in percent) which result from the information in Table 2 are: 2.4% (σ_2 set A) and 5.7% (σ_2 set B). The error is much larger for σ_2 set B because the shape differs much more drastically from σ_1 than does that for σ_2 set A.

Example 4

We shall now consider the same hypothetical data set as was treated in Example 3 (see Table 2), with the exception that non-vanishing correlations for the spectrum errors will be assumed. Again, both σ_2 set A and σ_2 set B are included.

First let us suppose that the uncertainties in the ϕ_i are 100%-correlated. The only way that this is possible is for each ϕ_i to be expressed as $\eta \xi_i$ where η is the common factor which must possess all the error (in other words, each ξ_i is without error). From Eq. 18, it is evident that the factor η cancels in the general expression for

R. As a consequence, no uncertainty in R is introduced by the uncertainty in the spectrum under these conditions (since the error is entirely attributed to the factor η). The solution to our problem is therefore trivial in the limit of complete correlation, i.e., there is no error in R due to the spectrum uncertainty.

In order to develop a non-trivial example, we have to assume that the off-diagonal correlations are other than either zero or unity. Let us assume then that all the off-diagonal coefficients of the correlation matrix corresponding to \bar{V}_ϕ are equal to 0.5 (50% correlation). Eq. 27 is required for this analysis. Since the associated computations are rather lengthy, a computer program has been written to expedite the task. The results of the calculation are: 1.7% (σ_2 set A) and 4.0% (σ_2 set B). As might be anticipated, these errors fall between zero for full correlation and the values obtained in Example 3 for no correlation.

It is tempting to generalize that the ratio error attributed to spectrum uncertainty decreases as the overall correlation increases. While this seems to be the case for the examples presented above, it would be imprudent to imply that this is always the case. In particular, we have not examined what occurs when anti-correlation (negative correlation coefficients) is encountered. We will pursue this matter no further here, but will simply suggest that care always be taken to perform the detailed calculations which are required before reaching any specific conclusions.

We will now turn our attention to the first term in Eq. 23. Proceeding formally in much the same fashion as was done above for the second term, we conclude that

$$(30) E_{R\sigma}^2 = \sum_i \sum_j (\partial R / \partial \sigma_i) V_{\sigma_{ij}} (\partial R / \partial \sigma_j).$$

No explicit indication is provided as to the specific nature and range of the indices "i" and "j". In fact, the summations must extend over both differential cross-section sets σ_1 and σ_2 . In order to make progress toward understanding the manner in which the cross-section uncertainties contribute to the error in R, and the role of the spectrum in this context, we choose here to make the assumption that the errors in σ_1 and σ_2 are uncorrelated. This assumption is not essential for a general application of the theory, but is merely a matter of convenience for explanatory purposes. Thus,

$$(31) E_{\sigma}^2 = E_{\sigma_1}^2 + E_{\sigma_2}^2,$$

with

$$(32) E_{R\sigma 1}^2 = \sum_{i=1}^n \sum_{j=1}^n (\partial R / \partial \sigma_{1i}) V_{\sigma 1ij} (\partial R / \partial \sigma_{1j}),$$

$$(33) E_{R\sigma 2}^2 = \sum_{i=1}^n \sum_{j=1}^n (\partial R / \partial \sigma_{2i}) V_{\sigma 2ij} (\partial R / \partial \sigma_{2j}).$$

$\bar{V}_{\sigma 1}$ and $\bar{V}_{\sigma 2}$ are submatrices of \bar{V}_{σ} situated along the diagonal. Zeros occupy the remaining locations in \bar{V}_{σ} . From Eq. 25 we are led to the formulas

$$(34) \partial R / \partial \sigma_{1i} = (-G_2 / G_1^2) \phi_i,$$

$$(35) \partial R / \partial \sigma_{2i} = (1 / G_1) \phi_i.$$

Consideration of Eqs. 32 through 35 yields the expressions

$$(36) E_{R\sigma 1}^2 = (G_2^2 / G_1^4) \sum_{i=1}^n \sum_{j=1}^n \phi_i V_{\sigma 1ij} \phi_j,$$

$$(37) E_{R\sigma 2}^2 = (1 / G_1^2) \sum_{i=1}^n \sum_{j=1}^n \phi_i V_{\sigma 2ij} \phi_j.$$

No loss in generality results if we limit further consideration to only one of these expressions. Thus, we focus attention on the effects of error in σ_1 as indicated by Eq. 36. Proceeding as we did above, we

first neglect correlations. Thus, $V_{\sigma 1ij} = E_{\sigma 1i}^2 \delta_{ij}$ where $E_{\sigma 1i}$ is the error in the group cross section σ_{1i} and δ_{ij} is the previously-defined Kronecker Delta Function. Then we obtain

$$(38) E_{R\sigma 1}^2 = (G_2^2 / G_1^4) \sum_{i=1}^n \phi_i^2 E_{\sigma 1i}^2.$$

This formula tells us what we wish to know about the nature of this term. As one is likely to suspect on the basis of intuition, the error in the ratio from this source comes from those portions of the energy range where the spectrum intensity is greatest, and where the errors in σ_1 are also significant. The square of the group flux ϕ_i serves as a weighting factor to determine the influence of the cross section uncertainty for the group in question. Therefore, even though the uncertainties in the spectrum have no influence here, the effective

uncertainty contribution represented by this term is certainly influenced indirectly by the detailed shape of the spectrum.

To illustrate the concepts we now consider two hypothetical examples. For each of these we turn to the spectrum and cross sections employed in the analysis appearing in Example 3 (see Table 2).

Example 5

Here we assume that each group cross section value σ_{1i} has an error of 10%, and that these are uncorrelated. Errors in ϕ and σ_2 are ignored for present purposes, so Eq. 38 is applicable for the computations. The hypothetical data utilized in the present calculations is similar to that used in previous examples. The essential parameters are reproduced in Table 3. The result of the analysis is an error of 4.1%. Table 3 also provides insight concerning the origins of this error. Most of the error contribution comes from Groups 1-6, as is evident from the entries under the column labelled $\phi_i^2 E_{\sigma_{1i}}$.

Example 6

Although our primary intent is not to examine the effects of cross section errors on the ratio, it is nevertheless interesting to examine how the computed error in the ratio changes if the errors in the cross sections are assumed to be correlated.

First, if the errors in the σ_{1i} are 100% correlated, it is evident from an argument similar to the one used in Example 4 that the corresponding ratio error is exactly 10%.

Partial correlation must now be considered in order to provide a non-trivial example. Once again, we will assume 50% correlation. The formula applicable to this analysis is Eq. 36, and a computer was used to complete the required calculations. The result is an error of 7.6%, smaller than that which is obtained in the case of full correlation but larger than the error determined when no correlation is included.

Example 7

We conclude this chapter by considering an example which utilizes actual data from the literature. For this purpose, we refer to the work of Watanabe et al. [13]. These authors have compared measured and calculated fission cross-section ratios for several fissionable isotopes in the fast-neutron spectrum generated by bombarding a thick Be-metal target with 7-MeV deuterons. Spectrum-average cross sections were computed using the method described in Ref. 14. Evaluated fission cross sections from ENDF/B-V [1] and two distinct representations of the neutron spectrum (obtained from Refs. 15 and 16, respectively) were

employed in this analysis. Some results are presented in Table 4. Comparison is made there between differences in the calculated integral ratios for the two distinct spectrum representations. Included in the table are ratios between fission processes having similar energy-differential behavior (e.g. N-N and T-T) and quite different energy-differential behavior (T-N). It is quite evident that the effects of differences in the spectrum representations (i.e., spectrum uncertainty) are more pronounced when the cross sections involved in the ratios differ considerably in their energy-differential behavior.

IV. CONCLUSIONS

The present investigation has produced methods for dealing with some important practical issues associated with the analysis of experimental and calculated reaction cross section ratios (e.g., the matter of assessing the utility of ratio data in evaluation applications).

For experiments involving quasi-monoenergetic neutron spectra, it has been shown by means of a perturbation analysis that measured ratio data can be converted to approximate point ("true" monoenergetic) values provided that estimates of the low-order moments of the spectrum and of certain parameters describing the energy dependence of the differential cross sections for the two reactions involved are available. Generally, the information required need not be very precisely known, and it can generally be acquired from a survey of the raw data and/or from prior knowledge derived from the literature.

When broad-energy spectra are involved, the impact of uncertainties in the spectral representations on the computation of integral cross section ratios can be readily analyzed by using covariance methods. With these it is possible to examine quantitatively the intuitively apparent result that spectrum-uncertainty effects become more acute when the energy-dependent behaviors of the differential cross sections differ considerably. The detail nature of the spectrum is also seen to be an important consideration in determining how differential cross section uncertainties are propagated through to the ratio error. In particular, large cross section errors have a significant effect whenever they correspond to an energy range which is strongly represented in the spectrum.

ACKNOWLEDGEMENTS

This work has been supported by the U.S. Department of Energy, Energy Research Programs, under contract W-31-109-Eng-38. The calculations discussed in Example 7, Chapter III, were performed by J.W. Meadows.

REFERENCES

1. "Evaluated Neutron Data File, ENDF/B-V", ENDF/B Summary Documentation, compiled by R. Kinsey, ENDF-201, 3rd Edition, Brookhaven National Laboratory (1979).
2. Donald L. Smith, "A Least-Squares Method for Deriving Reaction Differential Cross Section Information from Measurements Performed in Diverse Neutron Fields", ANL/NDM-77, Argonne National Laboratory (1982).
3. Y. Kanda and Y. Uenohara, "Some Activation Cross Sections Evaluated Simultaneously by Differential and Integral Measurements", International Conference on Neutron Physics, Kiev, U.S.S.R., September 21-25 (1987).
4. Donald L. Smith, "Some Comments on Resolution and the Analysis and Interpretation of Experimental Results from Differential Neutron Measurements", ANL/NDM-49, Argonne National Laboratory (1979).
5. D.L. Smith and J.W. Meadows, "Method of Neutron Activation Cross Section Measurement for $E_d = 5.5-10$ MeV Using the $D(d,n)^3\text{He}$ Reaction as a Neutron Source", ANL/NDM-9, Argonne National Laboratory (1974).
6. James W. Meadows and Donald L. Smith, "Neutron Source Investigations in Support of the Cross Section Program at the Argonne Fast-Neutron Generator", ANL/NDM-53, Argonne National Laboratory (1980).
7. Donald L. Smith, James W. Meadows, Manuel M. Bretscher and Samson A. Cox, "Cross-Section Measurement for the ${}^7\text{Li}(n,n't){}^4\text{He}$ Reaction at 14.74 MeV", ANL/NDM-87, Argonne National Laboratory (1984).
8. Roger L. Burford, Statistics: A Computer Approach, Charles E. Merrill Publishing Company, Columbus, Ohio (1968).
9. D.L. Smith, J.W. Meadows and M.M. Bretscher, "Integral Cross Section Measurements for ${}^7\text{Li}(n,n't){}^4\text{He}$, ${}^{27}\text{Al}(n,p){}^{27}\text{Mg}$, ${}^{27}\text{Al}(n,\alpha){}^{24}\text{Na}$, ${}^{58}\text{Ni}(n,p){}^{58}\text{Co}$ and ${}^{60}\text{Ni}(n,p){}^{60}\text{Co}$ Relative to ${}^{238}\text{U}$ Neutron Fission in the Thick-Target ${}^9\text{Be}(d,n){}^{10}\text{B}$ Spectrum at $E_d = 7$ MeV", ANL/NDM-93, Argonne National Laboratory (1985).
10. W. Mannhart, "Status of the ${}^{252}\text{Cf}$ Neutron Spectrum as a Standard", 6th ASTM/EURATOM Symposium on Reactor Dosimetry, Jackson Hole, Wyoming, 31 May-5 June, 1987.

11. Donald L. Smith, "Covariance Matrices and Applications to the Field of Nuclear Data", ANL/NDM-62, Argonne National Laboratory (1981).
12. Donald L. Smith, "Non-evaluation Applications for Covariance Matrices", ANL/NDM-67 (1982).
13. Y. Watanabe, J.W. Meadows and D.L. Smith, "An Integral Test of Several Fission Cross Sections in the Neutron Spectrum Produced by 7-MeV Deuterons Incident on a Thick Be-Metal Target", accepted for publication in *Annals of Nuclear Energy* (1987).
14. Donald L. Smith, "Analysis of the Sensitivity of Spectrum Average Cross Sections to Individual Characteristics of Differential Excitation Functions", ANL/NDM-30 (1977).
15. A. Crametz, H.-H. Knitter and D.L. Smith, "Thick-Target ${}^9\text{Be}(d,n){}^{10}\text{B}$ Neutron Spectrum at $E_d = 7$ MeV", Nuclear Data for Science and Technology, edited by K. Boekhoff, D. Reidel Publishing Company, Dordrecht, Holland, p. 902 (1983).
16. D.L. Smith, J.W. Meadows, P.T. Guenther and L.R. Greenwood, "Development of the Be(d,n) Neutron Source for Cross-Section Investigations in the Few-MeV Energy Range", 6th ASTM/EURATOM Symposium on Reactor Dosimetry, Jackson Hole, Wyoming, 31 May-5 June, 1987.

Table 1: Representation of the neutron spectrum from Example 1

i	E_i^a	ϕ_i^b	i	E_i^a	ϕ_i^b
1	5.617	0.02	16	5.821	0.76
2	5.631	0.04	17	5.834	0.83
3	5.644	0.07	18	5.848	0.92
4	5.658	0.11	19	5.861	1.00
5	5.671	0.14	20	5.875	0.99
6	5.685	0.18	21	5.888	0.94
7	5.699	0.23	22	5.902	0.85
8	5.712	0.26	23	5.915	0.73
9	5.726	0.32	24	5.929	0.62
10	5.739	0.37	25	5.943	0.50
11	5.753	0.42	26	5.956	0.38
12	5.766	0.48	27	5.970	0.26
13	5.780	0.55	28	5.983	0.13
14	5.793	0.61	29	5.997	0.02
15	5.807	0.68			

^a Neutron energy in MeV.

^b Relative neutron intensity (unnormalized spectrum).

Table 2: Numerical information associated with Example 3

i	ϕ_i^a	σ^b		A		B	
		σ_{1i}	σ_{2i}	$(\sigma_{2i} - \sigma_{1i})^2$	σ_{2i}	$(\sigma_{2i} - \sigma_{1i})^2$	
1	0.17405	28.9	4.913	5.754(2) ^c	0	8.352(2)	
2	0.20679	539.0	100.957	1.919(5)	0	2.905(5)	
3	0.19710	523.0	400.745	1.495(4)	0	2.735(5)	
4	0.16002	547.0	716.718	2.880(4)	0	2.992(5)	
5	0.12928	536.0	924.797	1.512(5)	1.625	2.856(5)	
6	0.06915	650.0	1094.343	1.974(5)	278.214	1.382(5)	
7	0.01724	935.0	1146.363	4.467(4)	2340.118	1.974(6)	
8	0.01670	992.0	1154.070	2.627(4)	5746.289	2.260(7)	
9	0.01563	997.0	1154.070	2.467(4)	9451.476	7.148(7)	
10	0.00902	982.0	1130.950	2.219(4)	12077.608	1.231(8)	
11	0.00501	987.0	1098.196	1.236(4)	14170.713	1.738(8)	

^a Spectrum is normalized, i.e. $\sum \phi_i = 1$.

^b All cross sections given in consistent arbitrary units.

^c $5.754(2) = 5.754 \times 10^2$.

Table 3: Numerical information associated with Example 5

i	ϕ_i^a	ϕ_i^2	σ_{1i}^b	$E_{\sigma 1i}^b$	$\phi_i^2 E_{\sigma 1i}^2$
1	0.17405	3.029(-2) ^c	28.9	2.89	0.253
2	0.20679	4.276(-2)	539.0	53.9	124.2
3	0.19710	3.885(-2)	523.0	52.3	106.3
4	0.16002	2.561(-2)	547.0	54.7	76.62
5	0.12928	1.671(-2)	536.0	53.6	48.02
6	0.06915	4.782(-3)	650.0	65.0	20.20
7	0.01724	2.972(-4)	935.0	93.5	2.598
8	0.01670	2.789(-4)	992.0	99.2	2.744
9	0.01563	2.443(-4)	997.0	99.7	2.428
10	0.00902	8.136(-5)	982.0	98.2	0.785
11	0.00501	2.510(-5)	987.0	98.7	0.245

^a Spectrum is normalized, i.e. $\sum \phi_i = 1$.

^b All cross sections and errors given in consistent arbitrary units.

^c $3.029(-2) = 3.029 \times 10^{-2}$.

Table 4: Numerical information associated with Example 7

Fission Ratio	Type ^a	Calculated Ratios		
		Spectrum 1 ^b	Spectrum 2 ^c	Difference (%)
$^{239}\text{Pu} : ^{235}\text{U}$	N-N	1.496	1.497	< 0.1
$^{232}\text{Th} : ^{238}\text{U}$	T-T	0.2609	0.2590	0.7
$^{238}\text{U} : ^{235}\text{U}$	T-N	0.3844	0.3763	2.1

^a N = non-threshold process. T = threshold process.

^b Be(d,n) spectrum measured by time of flight with a scintillation detector as described in Ref. 15.

^c Be(d,n) spectrum measured by time of flight using a fission detector as described in Ref. 16.

FIGURE CAPTION

Figure 1: Plot of $\sigma_1(E-E_0)$, $\sigma_2(E-E_0)$ and $\phi(E-E_0)$ as described in Chapter II, Example 1.

FIGURE 1

